

QUANTIFYING DISCORDANCE IN THE 2015 *PLANCK* CMB SPECTRUMG. E. ADDISON¹, Y. HUANG¹, D. J. WATTS¹, C. L. BENNETT¹, M. HALPERN², G. HINSHAW², AND J. L. WEILAND¹¹Dept. of Physics & Astronomy, The John Hopkins University, 3400 N. Charles St., Baltimore, MD 21218-2686, USA; gaddison@jhu.edu²Department of Physics and Astronomy, University of British Columbia, 6224 Agricultural Road, Vancouver, BC V6T 1Z1, Canada

Received 2015 October 30; accepted 2016 January 4; published 2016 February 16

ABSTRACT

We examine the internal consistency of the *Planck* 2015 cosmic microwave background (CMB) temperature anisotropy power spectrum. We show that tension exists between cosmological constant cold dark matter (Λ CDM) model parameters inferred from multipoles $\ell < 1000$ (roughly those accessible to *Wilkinson Microwave Anisotropy Probe*), and from $\ell \geq 1000$, particularly the CDM density, $\Omega_c h^2$, which is discrepant at 2.5σ for a *Planck*-motivated prior on the optical depth, $\tau = 0.07 \pm 0.02$. We find some parameter tensions to be larger than previously reported because of inaccuracy in the code used by the *Planck* Collaboration to generate model spectra. The *Planck* $\ell \geq 1000$ constraints are also in tension with low-redshift data sets, including *Planck*'s own measurement of the CMB lensing power spectrum (2.4σ), and the most precise baryon acoustic oscillation scale determination (2.5σ). The Hubble constant predicted by *Planck* from $\ell \geq 1000$, $H_0 = 64.1 \pm 1.7 \text{ km s}^{-1} \text{ Mpc}^{-1}$, disagrees with the most precise local distance ladder measurement of $73.0 \pm 2.4 \text{ km s}^{-1} \text{ Mpc}^{-1}$ at the 3.0σ level, while the *Planck* value from $\ell < 1000$, $69.7 \pm 1.7 \text{ km s}^{-1} \text{ Mpc}^{-1}$, is consistent within 1σ . A discrepancy between the *Planck* and South Pole Telescope high-multipole CMB spectra disfavors interpreting these tensions as evidence for new physics. We conclude that the parameters from the *Planck* high-multipole spectrum probably differ from the underlying values due to either an unlikely statistical fluctuation or unaccounted-for systematics persisting in the *Planck* data.

Key words: cosmic background radiation – cosmological parameters – cosmology: observations

1. INTRODUCTION

Measurements of the power spectrum of cosmic microwave background (CMB) temperature fluctuations (hereafter “TT spectrum”) are a cornerstone of modern cosmology. The most precise constraints are currently provided by the final 9 year *Wilkinson Microwave Anisotropy Probe* (WMAP) analysis (Bennett et al. 2013; Hinshaw et al. 2013), high-resolution, ground-based instruments including the Atacama Cosmology Telescope (ACT; Sievers et al. 2013) and the South Pole Telescope (SPT; Story et al. 2013), and most recently *Planck* (Planck Collaboration XIII 2015). Significant improvements in both CMB polarization and low-redshift, late-time observations are anticipated in the near future and will be used to measure or tightly constrain key cosmological quantities including the total neutrino mass, deviations of dark energy from a cosmological constant and the amplitude of primordial gravitational waves (e.g., Abazajian et al. 2013a, 2013b; Kim et al. 2013). Many of these future results will rely on having precise and accurate TT constraints. Assessing consistency both between and internally within each TT measurement is therefore extremely important.

While the *Planck* data from the first data release in 2013 (Planck Collaboration XVI 2014) were qualitatively in agreement with WMAP, supporting the minimal Λ CDM model, there were small but highly significant quantitative differences between the cosmological parameters inferred. For example, Larson et al. (2015) found a $\sim 6\sigma$ overall parameter discrepancy after accounting for the cosmic variance common to both experiments.

Several systematic effects were corrected in the *Planck* 2015 data release, including issues relating to data calibration and map making (Planck Collaboration I 2015), which led to a shift

in the inferred TT power spectrum amplitude by 3.5σ in units of the 2015 uncertainty (Table 1 of Planck Collaboration XIII 2015), and an artifact with a statistical significance of $2.4\text{--}3.1\sigma$ near multipole $\ell \simeq 1800$ in the 217 GHz temperature power spectrum (Planck Collaboration XII 2014). See also discussion in Spergel et al. (2015).

The WMAP and *Planck* 2015 TT spectra now appear to be in agreement over their common multipole range (Figure 46 of Planck Collaboration XI 2015). When the additional information in the high-order acoustic peaks and damping tail of the TT spectrum are included, however, the *Planck* parameters pull away from WMAP (Section 4.1.6 of Planck Collaboration XI 2015), leading to tension between *Planck* and several low-redshift cosmological measurements if Λ CDM is assumed, including a 2.5σ tension with the Riess et al. (2011) determination of the Hubble constant, H_0 , $2\text{--}3\sigma$ tension with weak lensing measurements of the CFHTLenS survey (Heymans et al. 2012), and tension with the abundance of massive galaxy clusters (e.g., Planck Collaboration XXIV 2015).

In this paper we examine the internal consistency of the *Planck* TT spectrum. We show that tension exists between Λ CDM parameters inferred from the *Planck* TT spectrum at the multipoles accessible to WMAP ($\ell \lesssim 1000$) and at higher multipoles ($\ell \gtrsim 1000$). The constraints from high multipoles are, furthermore, in tension with many low-redshift cosmological measurements, including *Planck*'s own lensing potential power spectrum measurement and baryon acoustic oscillation (BAO) from galaxy surveys, while the low-multipole *Planck* TT, *Planck* lensing, WMAP, BAO, and distance ladder H_0 data are all in reasonable agreement.

We describe the data sets used and parameter fitting methodology in Section 2 and present results in Section 3. Discussions and conclusions follow in Sections 4 and 5.

2. DATA AND PARAMETER FITTING

We use CAMB³ (Lewis et al. 2000) to calculate temperature and lensing potential power spectra as a function of cosmological parameters and CosmoMC⁴ (Lewis & Bridle 2002) to perform Monte-Carlo Markov Chain (MCMC) parameter fitting and obtain marginalized parameter distributions, adopting the default *Planck* settings, including a neutrino mass of 0.06 eV (Planck Collaboration XVI 2014). We use the public temperature-only *Planck* 2015 low ℓ likelihood for $2 \leq \ell \leq 29$, the binned plik likelihood for $30 \leq \ell \leq 2508$, and, in some cases, the *Planck* 2015 lensing likelihood, which includes multipoles of the lensing potential power spectrum $C_L^{\phi\phi}$ covering $40 \leq L \leq 400$ (Planck Collaboration XI 2015; Planck Collaboration XV 2015). We fit for six Λ CDM parameters: the physical baryon and CDM densities, $\Omega_b h^2$ and $\Omega_c h^2$; the angular acoustic scale, parametrized by θ_{MC} ; the optical depth, τ ; the primordial scalar fluctuation amplitude, A_s ; and the scalar spectral index, n_s . Other parameters, including H_0 , the total matter density, Ω_m , and the present-day mass fluctuation amplitude, σ_8 , are derived from these six parameters. Additional foreground and calibration parameters used in the fits are described by Planck Collaboration XI (2015).

At the present time the analysis of *Planck*'s polarization data is only partially complete. At high multipoles, significant systematic errors remain in the TE and EE spectra, putatively due to beam mismatch, which leads to temperature-polarization leakage (Section 3.3.2 of Planck Collaboration XIII 2015). At low multipoles ($\ell < 30$), the 100, 143, and 217 GHz polarization data have significant residual systematic errors and are “not considered usable for cosmological analyses.”⁵ The LFI 70 GHz data, in conjunction with the 30 and 353 GHz maps as Galactic foreground tracers, are used to constrain τ . Using the polarized 353 GHz map as a dust tracer results in a value of τ lower than constraints from WMAP (0.066 ± 0.016 compared to 0.089 ± 0.014 , Hinshaw et al. 2013; Planck Collaboration XIII 2015). Given these complexities and uncertainties, we have chosen to leave polarization data out of the current analysis and focus on conclusions that can be drawn from the TT data alone.

Without polarization data, τ is only weakly constrained, but it does couple to other cosmological parameters. We considered two approaches for setting priors on τ . First we adopted a Gaussian prior of $\tau = 0.07 \pm 0.02$ as in Planck Collaboration XI (2015), which is consistent within 1σ with the range of values inferred from WMAP and *Planck* data (Hinshaw et al. 2013; Planck Collaboration XIII 2015). Second, to gain more insight into exactly how τ does or does not affect our conclusions about TT consistency, we also ran chains with τ fixed to specific values: 0.06, 0.07, 0.08, and 0.09.

When assessing consistency between parameter constraints from two data sets that can be considered independent we use the difference of mean parameter values, which we treat as multivariate Gaussian with zero mean and covariance given by the sum of the covariance matrices from the individual data sets. The mean and covariance for each data set are estimated from the MCMC chains. We then quote equivalent Gaussian “sigma” levels for the significance of the parameter differences.

We also considered using the difference of best-fit parameters, rather than difference of means, for these comparisons. For Gaussian posterior distributions this choice should make little difference. We find that this is generally true, with significance levels for parameter differences changing only at the 0.1–0.2 σ level. In a few cases, however, we found a significant shift, due to an offset between the mean and best-fit parameters. In all cases the Gaussian distribution specified by the mean and covariance matrix from the chains provided an excellent match to the distribution of the actual MCMC samples, and for this reason we quote results based on the differences of the mean rather than best-fit parameters. It is possible that the mismatches are caused by problems in the algorithm used to determine the best-fit parameters.⁶ Note that simply taking the maximum-likelihood parameters directly from the MCMC chains is unreliable due to the large parameter volume sampled (typically around 20 parameters, including nuisance parameters, e.g., for foregrounds). The overall posterior distribution is well mapped out by a converged chain but the tiny region of parameter space close to the likelihood peak is not.

3. RESULTS

Figure 1 shows the two-dimensional Λ CDM parameter constraints for the *Planck* 2015 TT spectra spanning $2 \leq \ell < 1000$ and $1000 \leq \ell \leq 2508$, with a $\tau = 0.07 \pm 0.02$ prior. Similar contours are shown in Figure 31 of Planck Collaboration XI (2015) using the same prior on τ . Two differences in our fit act to pull some of the low and high multipole parameter constraints away from one another. First, the constraints in the *Planck* figure only extend down to $\ell = 30$ because the intention was to test the robustness of the plik likelihood only. We use the full range $2 \leq \ell < 1000$ with the intention of examining parameter values. Second, the *Planck* fit uses the PICO⁷ (Fendt & Wandelt 2007) code rather than CAMB to generate TT spectra. We find that the PICO and CAMB results are noticeably different for the $1000 \leq \ell \leq 2508$ fit. PICO requires only a fraction of the computation time and provides a good approximation to CAMB, but only within a limited volume of parameter space. Some parameter combinations outside this volume are allowed by the $1000 \leq \ell \leq 2508$ data. In these cases, the PICO output deviates from the CAMB spectrum and a poor likelihood is returned, leading to artificial truncation of the contours, particularly for $\Omega_b h^2$ and n_s .

From Figure 1 it is clear that some tension exists between parameters inferred from the $\ell < 1000$ and $\ell \geq 1000$ *Planck* TT spectra. Assuming the two sets of constraints are independent, the values of $\Omega_c h^2$ differ by 2.5σ . Independence is a valid assumption because even the bins on either side of the $\ell = 1000$ split point are only correlated at the 4% level and the degree of correlation falls off with increasing bin separation. Taken together the five free Λ CDM parameters differ by 1.8σ , however it should be noted that $\Omega_c h^2$ plays a far more significant role in comparisons with low-redshift cosmological constraints (Section 3.3) than, for example, θ_{MC} .

For fixed τ we find differences in $\Omega_c h^2$ of 3.0, 2.7, 2.9, and 2.1 σ for τ values of 0.06, 0.07, 0.08, and 0.09, respectively. Constraints on each parameter for these cases are shown in

³ camb.info

⁴ <http://cosmologist.info/cosmomc/>

⁵ According to the *Planck* 2015 Release Explanatory Supplement http://wiki.cosmos.esa.int/planckpla2015/index.php/Frequency_Maps#Caveats_and_known_issues.

⁶ See <http://cosmologist.info/cosmomc/readme.html>.

⁷ <https://pypi.python.org/pypi/pycico>

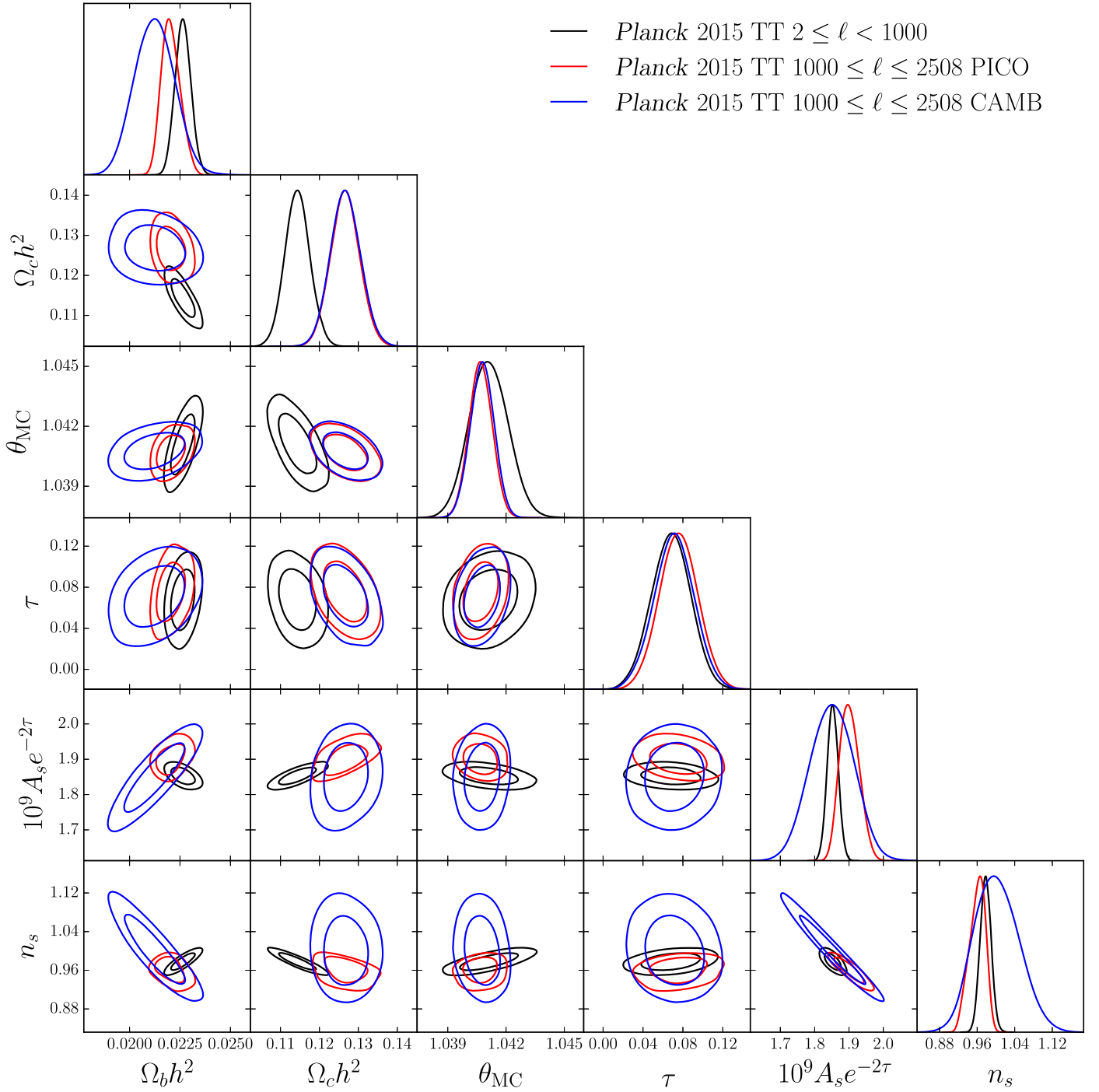


Figure 1. Contours enclosing 68.3% and 95.5% of MCMC sample points from fits to the *Planck* TT spectrum. Results are shown for $2 \leq \ell < 1000$, roughly the multipole range accessible to *WMAP*, and higher multipoles, $1000 \leq \ell \leq 2508$. These constraints are effectively independent and are in tension, for example $\Omega_c h^2$ differs by 2.5σ . Results are also shown for the $1000 \leq \ell \leq 2508$ fit where the PICO code is used to estimate the theoretical TT spectra instead of the more accurate CAMB. Using PICO leads to an artificial truncation of the contours and diminishes the discrepancy between the high and low multipole fits for some parameters. We adopt a Gaussian prior of $\tau = 0.07 \pm 0.02$.

Figure 2. Apart from the expected strong correlation with A_s (the TT power spectrum amplitude scales as $A_s e^{-2\tau}$) there is relatively little variation with τ . Note that while increasing τ reduces the tension in $\Omega_c h^2$, higher values of τ are mildly disfavored by *Planck*'s own polarization analysis (Planck Collaboration XIII 2015).

We investigated the effect of fixing the foreground parameters to the best-fit values inferred from the fit to the

whole *Planck* multipole range rather than allowing them to vary separately in the $\ell < 1000$ and $\ell \geq 1000$ fits. This helps break degeneracies between foreground and Λ CDM parameters and leads to small shifts in Λ CDM parameter agreement, with the tension in $\Omega_c h^2$ decreasing to 2.3σ for $\tau = 0.07 \pm 0.02$, for example. The best-fit χ^2 is, however, worse by 3.1 and 4.8 for the $\ell < 1000$ and $\ell \geq 1000$ fits, respectively, reflecting the fact that the $\ell < 1000$ and $\ell \geq 1000$ data mildly prefer different

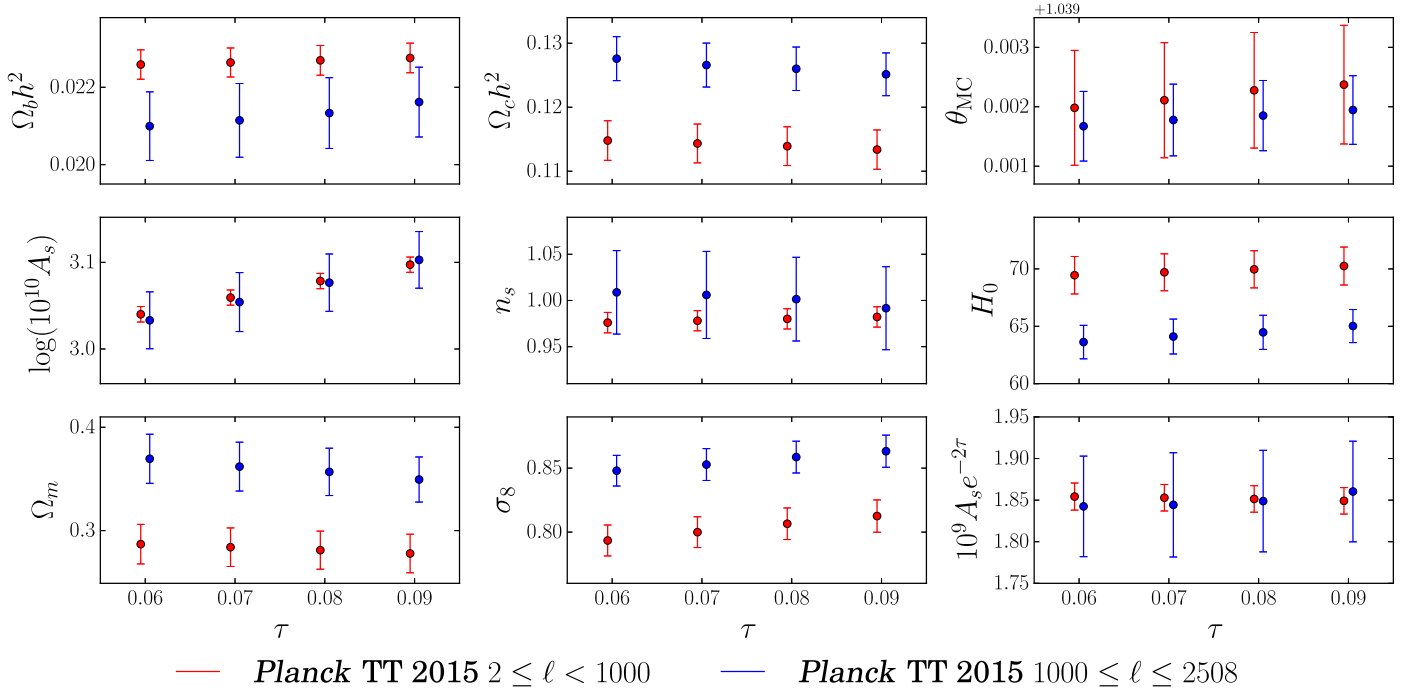


Figure 2. Marginalized 68.3% confidence Λ CDM parameter constraints from fits to the $\ell < 1000$ and $\ell \geq 1000$ *Planck* TT spectra. Here we replace the prior on τ with fixed values of 0.06, 0.07, 0.08, and 0.09, to more clearly assess the effect τ has on other parameters in these fits. Aside from the strong correlation with A_s , which arises because the TT spectrum amplitude scales as $A_s e^{-2\tau}$, dependence on τ is fairly weak. Tension at the $>2\sigma$ level is apparent in $\Omega_c h^2$ and derived parameters, including H_0 , Ω_m , and σ_8 .

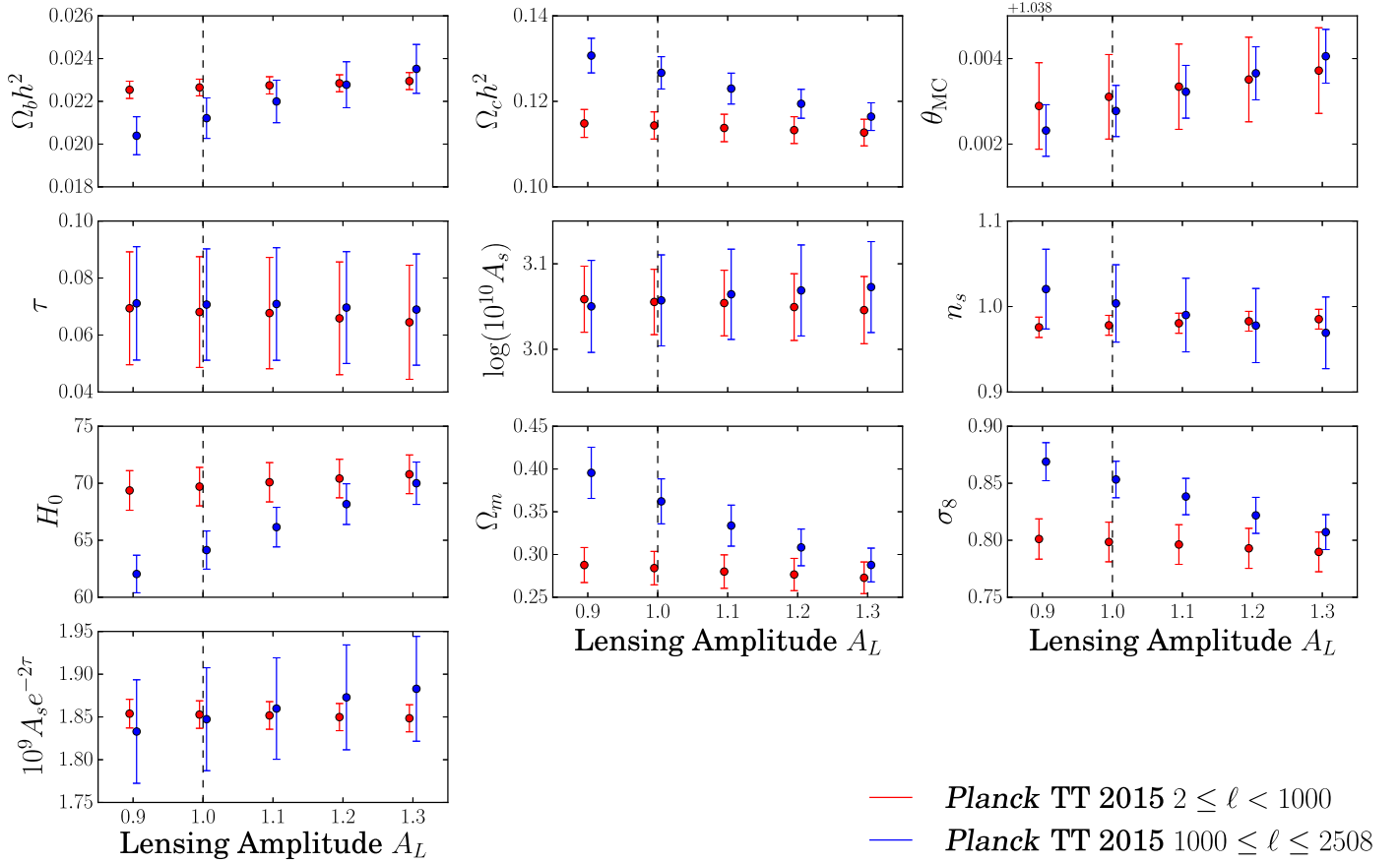


Figure 3. Marginalized 68.3% parameter constraints from fits to the $\ell < 1000$ and $\ell \geq 1000$ *Planck* TT spectra with different values of the phenomenological lensing amplitude parameter, A_L , which has a physical value of unity (dashed line). Increasing A_L smooths out the high order acoustic peaks, which improves agreement between the two multipole ranges. Note that a high value of A_L is not favored by the direct measurement of the $\phi\phi$ lensing potential power spectrum (see text).

foreground parameters. Overall the choice of foreground parameters does not significantly impact our conclusions.

3.1. Comparing Temperature and Lensing Spectra

Planck Collaboration XIII (2015) found that allowing a non-physical enhancement of the lensing effect in the TT power spectrum, parametrized by the amplitude parameter A_L (Calabrese et al. 2008), was effective at relieving the tension between the low and high multipole *Planck* TT constraints. For the range of scales covered by *Planck*, the main effect of increasing A_L is to slightly smooth out the acoustic peaks. If Λ CDM parameters are fixed, then a 20% change in A_L suppresses the fourth and higher peaks by around 0.5% and raises troughs by around 1%, for example.

In Figure 3 we show the effect of fixing A_L to values other than the physical value of unity on the $\ell < 1000$ and $\ell \geq 1000$ parameter comparison, for $\tau = 0.07 \pm 0.02$. For $A_L > 1$ the parameters from $\ell \geq 1000$ shift toward the $\ell < 1000$ results, resulting in lower values of $\Omega_c h^2$ and higher values of H_0 . Planck Collaboration XIII (2015) found $A_L = 1.22 \pm 0.10$ for *plik* combined with the low- ℓ *Planck* joint temperature and polarization likelihood, although note that this fit was performed using PICO rather than CAMB, which uses a somewhat different A_L definition.

Lensing also induces specific non-Gaussian signatures in CMB maps that can be used to recover the lensing potential power spectrum (hereafter “ $\phi\phi$ spectrum”). Planck Collaboration XV (2015) report a measurement of the $\phi\phi$ spectrum using temperature and polarization data with a combined significance of $\sim 40\sigma$. The $\phi\phi$ spectrum constrains $\sigma_8 \Omega_m^{0.25} = 0.591 \pm 0.021$, assuming priors of $\Omega_b h^2 = 0.0223 \pm 0.0009$, $n_s = 0.96 \pm 0.02$, and $0.4 < H_0/100 \text{ km s}^{-1} \text{ Mpc}^{-1} < 1.0$ (Planck Collaboration XV 2015). We computed constraints on this same parameter combination from *Planck* TT data using a $\tau = 0.07 \pm 0.02$ prior:

$$\begin{aligned} \sigma_8 \Omega_m^{0.25} &= 0.591 \pm 0.021 \text{ (Planck 2015 } \phi\phi\text{)}, \\ &= 0.583 \pm 0.019 \text{ (Planck 2015 TT } \ell < 1000\text{)}, \\ &= 0.662 \pm 0.020 \text{ (Planck 2015 TT } \ell \geq 1000\text{)}. \end{aligned} \quad (1)$$

The $\ell < 1000$ and $\ell \geq 1000$ TT values differ by 2.9σ , consistent with the difference in $\Omega_c h^2$ discussed above. The $\ell \geq 1000$ and $\phi\phi$ values are in tension at the 2.4σ level (for fixed values of τ in the range 0.06–0.09 we find a 2.4–2.5 σ difference). The $\ell < 1000$ TT and $\phi\phi$ values are consistent within 0.3σ .

It is worth noting that while allowing $A_L > 1$ does relieve tension between the low- ℓ and high- ℓ TT results, it does not alleviate the high- ℓ TT tension with $\phi\phi$. For $A_L = 1.2$ (by the CAMB definition) we find $\sigma_8 \Omega_m^{0.25} = 0.612 \pm 0.019$ from $\ell \leq 1000$, while the $\phi\phi$ spectrum requires $\sigma_8 \Omega_m^{0.25} = 0.541 \pm 0.019$. This is because the $\phi\phi$ power roughly scales as $A_L (\sigma_8 \Omega_m^{0.25})^2$, so, for fixed $\phi\phi$, increasing A_L by 20% requires a $\sim 10\%$ decrease in $\sigma_8 \Omega_m^{0.25}$. As shown in Figure 4, there is no value of A_L that produces agreement between these data.

The $\phi\phi$ spectrum featured prominently in the *Planck* claim that the true value of τ is lower than the value inferred by *WMAP* (Planck Collaboration XIII 2015). While a full investigation into τ is deferred to future work we note here that the effect of the $\phi\phi$ spectrum on τ is completely dependent

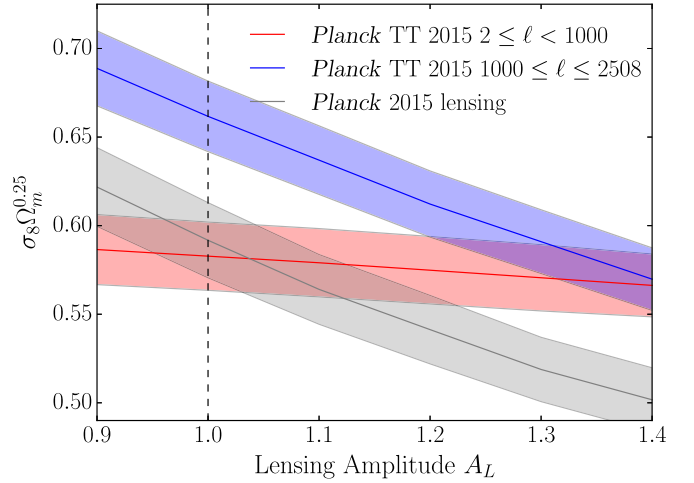


Figure 4. Constraints on $\sigma_8 \Omega_m^{0.25}$ from fits to the $\ell < 1000$ and $\ell \geq 1000$ *Planck* TT spectra, and to the *Planck* $\phi\phi$ lensing spectrum. Results are shown as a function of the phenomenological lensing amplitude parameter A_L . The $\phi\phi$ measurement constrains the product $A_L (\sigma_8 \Omega_m^{0.25})^2$. A similar trend is apparent in the $\ell \geq 1000$ constraint, where lensing has a significant effect. For $\ell < 1000$ the lensing effect is small, resulting in almost no dependence on A_L . The $\ell < 1000$ and $\phi\phi$ constraints agree well for the physical value of $A_L = 1$ (dashed line). Increasing A_L helps reconcile the low- ℓ and high- ℓ constraints but does not improve agreement between the high- ℓ and $\phi\phi$ constraints.

on the choice of temperature and polarization data. The shift to lower τ in the joint *Planck* 2015 TT- $\phi\phi$ fit is partly a reflection of the tension discussed above. Adding the *Planck* $\phi\phi$ spectrum to the *WMAP*9 data, in contrast, leads to no measurable shift in τ at all, reflecting the fact that the $\phi\phi$ spectrum and *WMAP* temperature and polarization data (with $\tau = 0.089 \pm 0.014$) are in excellent agreement. Figure 5 shows that, while some parameter constraints are tightened by a factor of two over *WMAP* alone, the mean values shift by $< 0.25\sigma$.

3.2. Comparison With SPT

Planck Collaboration XVI (2014) reported moderate to strong tension between cosmological parameters from the SPT TT spectrum, measured over 2500 square degrees and covering $650 \leq \ell \leq 3000$ (Story et al. 2013), and the *Planck* TT spectrum. Planck Collaboration XIII (2015) comment that this tension has worsened for the *Planck* 2015 data. A detailed comparison of these data sets is beyond the scope of this work, however, we note that when we recalibrate the public SPT spectrum to the full-sky *Planck* 2015 spectrum following the method described by Story et al. (2013), using data from $650 \leq \ell \leq 1000$ and correcting for foregrounds, we recover the original SPT calibration to *WMAP* within 0.3σ . For the 143 GHz *Planck* spectrum, most directly comparable to the 150 GHz SPT channel, the agreement is better than 0.1σ . The disagreement between SPT and *Planck* therefore cannot be resolved by simply calibrating SPT to *Planck* rather than *WMAP* in this manner. We note that the high-multipole ACT TT measurements are consistent with *WMAP* and SPT, as well as *Planck* 2013 if a recalibration is allowed (Calabrese et al. 2013; Louis et al. 2014), and so do not currently help our understanding of these tensions. More precise upcoming measurements from ACTPol will be useful for future comparisons.

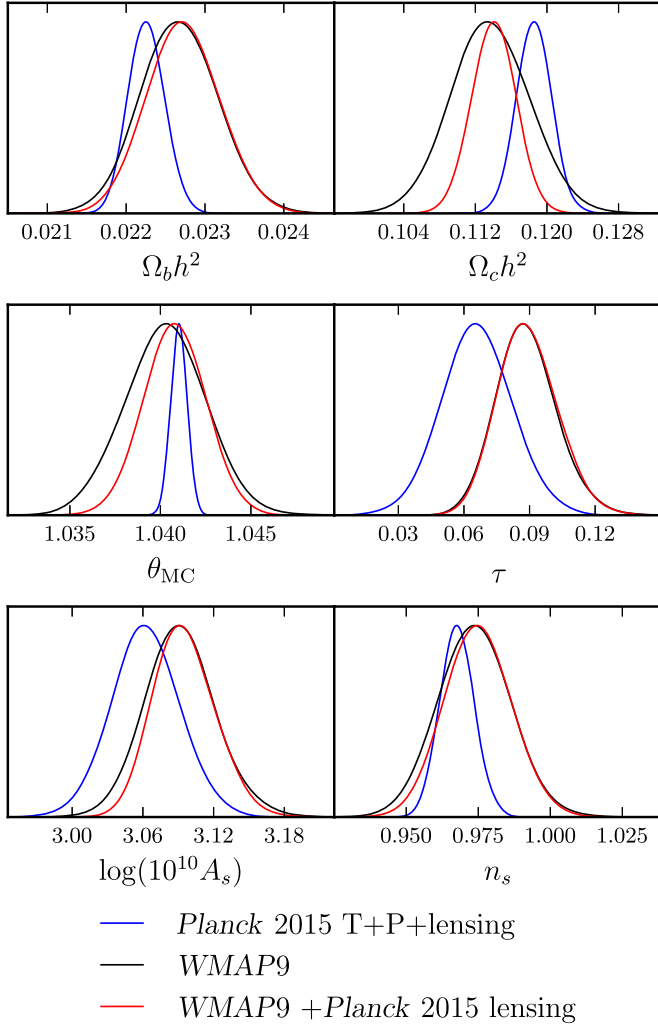


Figure 5. Marginalized Λ CDM parameter constraints comparing results from *Planck* 2015 (combined temperature, polarization and lensing) with *WMAP*9 alone and *WMAP*9 in conjunction with the *Planck* $\phi\phi$ lensing power spectrum. Adding the $\phi\phi$ spectrum to *Planck* temperature and polarization data results in a downward shift in τ , which reflects internal tension between the high-multipole *Planck* TT spectrum and $\phi\phi$ (see text). The *WMAP*9 and *Planck* $\phi\phi$ constraints are in very good agreement. Adding $\phi\phi$ to *WMAP* leads to a negligible shift in τ and shifts of $<0.25\sigma$ in other parameters.

3.3. Comparison With BAO and Local H_0 Measurements

Figure 6 shows a comparison of CMB Λ CDM constraints with the 1% BAO scale measurement from the Baryon Oscillation Spectroscopic Survey (BOSS) “CMASS” galaxy sample at an effective $z = 0.57$ (Anderson et al. 2014) and the most precise local distance ladder constraint on the Hubble constant, $H_0 = 73.0 \pm 2.4 \text{ km s}^{-1} \text{ Mpc}^{-1}$ (Riess et al. 2011; Bennett et al. 2014). The BAO scale is parametrized as the ratio of the combined radial and transverse dilation scale, D_V (Eisenstein et al. 2005), to the sound horizon at the drag epoch, r_d , which has a fiducial value $r_{d,\text{fid}} = 149.28 \text{ Mpc}$ (Anderson et al. 2014).

The BOSS BAO D_V/r_d constraint is at the higher end of the range preferred by *WMAP* and *Planck* $\ell < 1000$, though consistent within 1σ . The *Planck* $\ell \geq 1000$ data predict higher values of D_V/r_d , and lower values of H_0 , than the BOSS BAO and distance ladder measurements at the 2.5σ and 3.0σ level, respectively, for $\tau = 0.07 \pm 0.02$. The difference between the

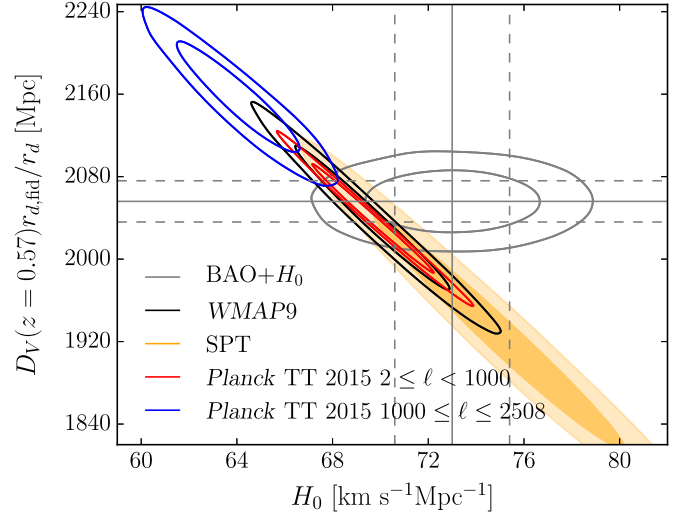


Figure 6. BOSS BAO scale and local distance ladder H_0 measurements (Riess et al. 2011; Anderson et al. 2014; Bennett et al. 2014) with Λ CDM CMB 68.3 and 94.5% confidence contours overplotted. The *Planck* $\ell \geq 1000$ constraints are discrepant with the BAO and distance ladder measurements at the 2.5σ and 3.0σ levels, respectively, while the *WMAP*9 and *Planck* $\ell < 1000$ constraints are consistent with both within 1σ . Constraints from SPT (covering $650 \leq \ell \leq 3000$) are also shown. *Planck* and SPT currently provide the most precise measurements of the CMB damping tail and their predictions for the $z = 0.57$ BAO scale and H_0 differ at the 2.6σ and 2.7σ level.

Planck high-multipole constraint and the Riess et al. (2011) H_0 constraint is extremely unlikely to be explained by statistical fluctuation alone. The SPT-only values provided by Story et al. (2013)⁸ are also shown. The SPT predictions for D_V/r_d and H_0 are discrepant with those from *Planck* $\ell \geq 1000$ at the 2.6σ and 2.7σ levels. Note that SPT used a *WMAP*-based τ prior but that τ couples very weakly to the inferred BAO scale.

The consistency between the *Planck* and BAO constraints has been repeatedly highlighted (Planck Collaboration XVI 2014; Planck Collaboration XIII 2015). We find that this agreement arises more in spite of than because of the high-multipole TT spectrum that *WMAP* did not measure. Figure 7 shows constraints in the $\Omega_m - H_0$ plane for the BAO constraint from combining BOSS CMASS with the BOSS “LOWZ” sample (Anderson et al. 2014), Sloan Digital Sky Survey Main Galaxy Sample (Ross et al. 2015, SDSS MGS), and Six-degree-Field Galaxy Survey (Beutler et al. 2011, 6dFGS) measurements. This is the same combination utilized in the *Planck* 2015 cosmological analysis. The BAO contours are plotted assuming $\Omega_b h^2 = 0.02223$, although the exact choice has little effect (Addison et al. 2013; Bennett et al. 2014). CMB constraints are plotted for comparison. The $>2\sigma$ tension between the *Planck* $\ell \geq 1000$ and BOSS BAO constraints persists with the full BAO data set.

Bennett et al. (2014) combined *WMAP*9, ACT, SPT, BAO, and distance ladder measurements and found that these measurements are consistent and together constrain $H_0 = 69.6 \pm 0.7 \text{ km s}^{-1} \text{ Mpc}^{-1}$. This concordance value differs from the *Planck* $\ell \geq 1000$ constraint of $64.1 \pm 1.7 \text{ km s}^{-1} \text{ Mpc}^{-1}$ at 3.1σ but agrees well with the *Planck* $\ell < 1000$ constraint of $69.7 \pm 1.7 \text{ km s}^{-1} \text{ Mpc}^{-1}$.

⁸ <http://pole.uchicago.edu/public/data/story12/chains/>

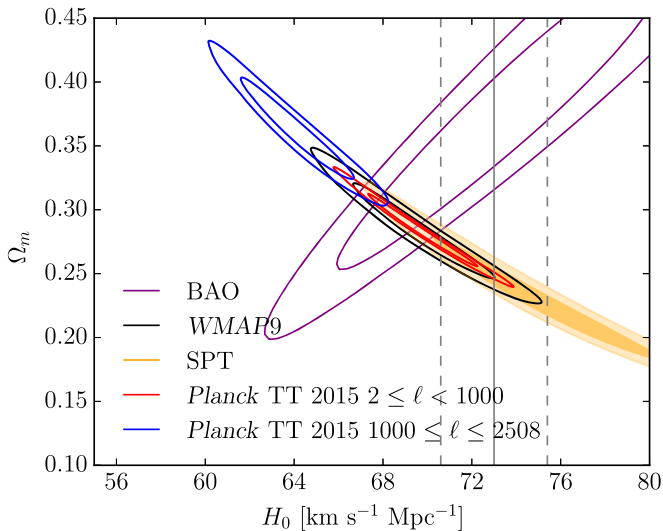


Figure 7. Comparison of CMB, BAO, and distance ladder constraints in the $\Omega_m - H_0$ plane. We show here the BAO constraints from combining the BOSS CMASS, BOSS LOWZ, SDSS MGS, and 6dFGRS measurements, assuming $\Omega_b h^2 = 0.0223$ (see text). The tension between *Planck* $\ell \geq 1000$ and BOSS CMASS BAO (Figure 6) persists when comparing to the joint BAO constraint.

3.4. Choice of Multipole Split

The choice of $\ell = 1000$ as the split point for parameter comparisons matches the tests described by Planck Collaboration XI (2015) and roughly corresponds to the maximum multipoles accessible to *WMAP*, but the exact choice is arbitrary. To test the robustness of our findings, we also considered the effect of splitting the *Planck* TT spectrum at $\ell = 800$. This choice achieves an almost even division of the *Planck* TT spectrum constraining power as assessed by the determinants of the Λ CDM parameter covariance matrices from fits to $2 \leq \ell \leq 799$ and $800 \leq \ell \leq 2508$, which differ by only a few per cent.

Adding the $800 \leq \ell < 1000$ range, including the third acoustic peak, to the high-multipole *Planck* fit has a significant effect on several parameters, including n_s and $\Omega_b h^2$, tightening constraints on these parameters by factors of four and two, respectively. Conversely, the uncertainty on θ_{MC} is increased by 50% for $\ell \leq 800$ compared to $\ell \leq 1000$. Despite these changes, the tensions discussed above for a split at $\ell = 1000$ remain for a split at $\ell = 800$, with the 2.5σ tension in $\Omega_c h^2$ for the $\ell = 1000$ split shifting to 2.7σ for the $\ell = 800$ case (assuming a $\tau = 0.07 \pm 0.02$ prior). From $\ell \geq 800$ we find $\sigma_8 \Omega_m^{0.25} = 0.657 \pm 0.018$, which is higher than the *Planck* $\phi\phi$ constraint in Equation (1) by 2.4σ , the same difference as for $\ell \geq 1000$. We conclude that the particular choice of $\ell = 1000$ is not driving our results.

4. DISCUSSION

We have found multiple similar tensions at the $>2\sigma$ level between the *Planck* 2015 high-multipole TT power spectrum and a range of other measurements. In general such tensions could be due to (i) statistical fluctuations, (ii) an incorrect cosmological model, or (iii) systematic errors or underestimation of statistical errors in the *Planck* spectrum. A combination of these factors is also possible.

If the tensions were largely due to an unlikely statistical fluctuation, our results suggest that it is parameters from the

high-multipole *Planck* TT spectrum that have scattered unusually far from the underlying values, on the basis that the low-multipole *Planck* TT, *WMAP*, *Planck* $\phi\phi$, BAO, and distance ladder H_0 measurements are all in reasonable agreement with one another (see also Bennett et al. 2014). One might argue that the $\ell < 1000$ *WMAP* and *Planck* constraints are pulled away from the true values by the multipoles at $\ell < 30$. However, all parameter constraints we have quoted include cosmic variance uncertainty and thus account for this possibility (assuming Gaussian fluctuations). Furthermore, an unusual statistical fluctuation in the $\ell < 1000$ values cannot explain the disagreement between the *Planck* $\ell \geq 1000$ constraints and SPT, *Planck* $\phi\phi$, BAO, and the distance ladder measurements.

Cosmology beyond standard Λ CDM cannot be ruled out as the dominant cause of tension. We do not favor this explanation because, first, none of the physically motivated modifications investigated by Planck Collaboration XIII (2015) were found to be significantly preferred in fits to the full *Planck* TT spectrum, and, second, the most precise measurements of the CMB damping tail, from *Planck* and SPT, disagree, as discussed in Sections 3.2 and 3.3.

From 2013 to 2015 the *Planck* results were revised due to several significant systematic effects. Without more detailed reanalysis of the *Planck* 2015 data we are not in a position to comment on remaining sources of systematic error in the *Planck* high-multipole spectrum. We do note that the TT covariance matrices described in Planck Collaboration XIII (2015) were calculated analytically assuming that sky components are Gaussian. Both foregrounds and the primary CMB have known non-Gaussian characteristics (in the latter case due to lensing, see, e.g., Benoit-Lévy et al. 2012) that would result in this approximation underestimating the true TT spectrum uncertainties, particularly at high multipoles where the foreground power becomes comparable to the CMB signal and the lensing effect is most important.

Finally, we emphasize that, irrespective of what is responsible for these tensions, care must clearly be taken when interpreting joint fits including the full range of *Planck* multipoles, particularly given *Planck*'s high precision and ability to statistically dominate other measurements, regardless of accuracy.

5. CONCLUSIONS

We have discussed tensions between the *Planck* 2015 high-multipole TT spectrum ($\ell \geq 1000$, roughly the scales inaccessible to *WMAP*) and the cosmological measurements:

- (i) the *Planck* 2015 TT spectrum at $\ell < 1000$, which prefers a value of $\Omega_c h^2$ 2.5σ lower than the high-multipole fit,
- (ii) the *Planck* 2015 $\phi\phi$ lensing power spectrum, which has an amplitude (parametrized by $\sigma_8 \Omega_m^{0.25}$) 2.4σ lower than predicted from the $\ell \geq 1000$ TT spectrum,
- (iii) the SPT TT spectrum, covering $650 \leq \ell \leq 3000$, which predicts, for example, a Hubble constant 2.7σ higher than *Planck* $\ell \geq 1000$,
- (iv) the most precise measurement of the BAO scale, from the BOSS CMASS galaxy sample at effective redshift $z = 0.57$, which disagrees at the 2.5σ level, and
- (v) the most precise local distance ladder determination of H_0 , which is in tension at the 3.0σ level.

These differences are quoted assuming $\tau = 0.07 \pm 0.02$. We found that some tensions are reduced by allowing larger values of τ but note that this would introduce new tension with *Planck* polarization data. Definitive conclusions about τ will require a more detailed understanding of low- ℓ foreground contamination. The Cosmology Large Angular Scale Surveyor is expected to provide a cosmic variance limited measurement of τ (Essinger-Hileman et al. 2014; Watts et al. 2015).

Given these results and the previously reported tensions with some weak lensing and cluster abundance data, we suggest that the parameter constraints from the high-multipole *Planck* data appear anomalous due to either an unlikely statistical fluctuation, remaining systematic errors, or both. Understanding the origin of these discrepancies is important given the role *Planck* data might play in future cosmological advances.

We are grateful to Adam Riess for reading the manuscript and providing helpful comments. We also thank Erminia Calabrese and Karim Benabed for help with *CosmoMC* and the *Planck* likelihood code, respectively. This research was supported in part by NASA grant NNX14AF64G and by the Canadian Institute for Advanced Research (CIFAR). We acknowledge the use of the Legacy Archive for Microwave Background Data Analysis (LAMBDA). This work was based on observations obtained with *Planck* (<http://www.esa.int/Planck>), an ESA science mission with instruments and contributions directly funded by ESA Member States, NASA, and Canada. Part of this research project was conducted using computational resources at the Maryland Advanced Research Computing Center (MARCC).

REFERENCES

- Abazajian, K. N., Arnold, K., Austermann, J., et al. 2013a, arXiv:1309.5381
 Abazajian, K. N., Arnold, K., Austermann, J., et al. 2013b, arXiv:1309.5383
 Addison, G. E., Hinshaw, G., & Halpern, M. 2013, *MNRAS*, 436, 1674
 Anderson, L., Aubourg, É., Bailey, S., et al. 2014, *MNRAS*, 441, 24
 Bennett, C. L., Larson, D., Weiland, J. L., & Hinshaw, G. 2014, *ApJ*, 794, 135
 Bennett, C. L., Larson, D., Weiland, J. L., et al. 2013, *ApJS*, 208, 20
 Benoit-Lévy, A., Smith, K. M., & Hu, W. 2012, *PhRvD*, 86, 123008
 Beutler, F., Blake, C., Colless, M., et al. 2011, *MNRAS*, 416, 3017
 Calabrese, E., Hlozek, R. A., Battaglia, N., et al. 2013, *PhRvD*, 87, 103012
 Calabrese, E., Slosar, A., Melchiorri, A., Smoot, G. F., & Zahn, O. 2008, *PhRvD*, 77, 123531
 Eisenstein, D. J., Zehavi, I., Hogg, D. W., et al. 2005, *ApJ*, 633, 560
 Essinger-Hileman, T., Ali, A., Amiri, M., et al. 2014, *Proc. SPIE*, 9153, 1
 Fendt, W. A., & Wandelt, B. D. 2007, *ApJ*, 654, 2
 Heymans, C., Van Waerbeke, L., Miller, L., et al. 2012, *MNRAS*, 427, 146
 Hinshaw, G., Larson, D., Komatsu, E., et al. 2013, *ApJS*, 208, 19
 Kim, A., Padmanabhan, N., Aldering, G., et al. 2013, arXiv:1309.5382
 Larson, D., Weiland, J. L., Hinshaw, G., & Bennett, C. L. 2015, *ApJ*, 801, 9
 Lewis, A., & Bridle, S. 2002, *PhRvD*, 66, 103511
 Lewis, A., Challinor, A., & Lasenby, A. 2000, *ApJ*, 538, 473
 Louis, T., Addison, G. E., Hasselfield, M., et al. 2014, *JCAP*, 7, 16
 Planck Collaboration XII 2014, *A&A*, 571, A12
 Planck Collaboration XVI 2014, *A&A*, 571, A16
 Planck Collaboration I 2015, arXiv:1502.01582
 Planck Collaboration XI 2015, arXiv:1507.02704
 Planck Collaboration XIII 2015, arXiv:1502.01589
 Planck Collaboration XV 2015, arXiv:1502.01591
 Planck Collaboration XXIV 2015, arXiv:1502.01597
 Riess, A. G., Macri, L., Casertano, S., et al. 2011, *ApJ*, 730, 119
 Ross, A. J., Samushia, L., Howlett, C., et al. 2015, *MNRAS*, 449, 835
 Sievers, J. L., Hlozek, R. A., Nolte, M. R., et al. 2013, *JCAP*, 10, 60
 Spergel, D. N., Flauger, R., & Hlozek, R. 2015, *PhRvD*, 91, 023518
 Story, K. T., Reichardt, C. L., Hou, Z., et al. 2013, *ApJ*, 779, 86
 Watts, D. J., Larson, D., Marriage, T. A., et al. 2015, *ApJ*, 814, 103